

## WEST COAST WINTER CYCLOGENESIS

Gary M. Lackmann

*Department of Marine, Earth, and Atmospheric Sciences  
North Carolina State University, Raleigh, North Carolina***1. INTRODUCTION**

During outbreaks of arctic air over western North America, an inverted trough is often observed along the coast of British Columbia and the U.S. Pacific Northwest. Occasionally, coastal cyclogenesis can take place within this vorticity-rich coastal environment, and these systems can occasionally bring heavy snow to the interior sections of western Washington and Oregon. The complex environment in which these cyclones develop includes influences from coastal processes, topography, diabatic processes, and synoptic-scale dynamics. The purpose of this research is to investigate the relative importance of topography, diabatic processes, and upper-tropospheric dynamics for a coastal cyclone event that took place during January, 1980.

The inverted coastal trough (e.g., Fig. 1), which has been discussed by Lackmann and Overland (1989) and Ferber et al. (1993), can be conceptualized as the result of geostrophic adjustment in a down-gradient ageostrophic flow that develops in the presence of an along-barrier pressure-gradient force (e.g., Bailey et al. 2003). Once formed, this trough provides a vorticity-rich environment in which cyclogenesis is favored. In addition to the topographic component, the trough is characterized by strong baroclinicity, especially during winter. This is due in part to differential diabatic heating between land to the east of the trough axis and the warm oceanic lower boundary to the west. These characteristics make the inverted trough a potential site for coastal cyclogenesis; however, these West Coast events often feature upper-level ridging to the west of the area (e.g., Fig. 1). This blocking ridge tends to limit the frequency of mobile upper troughs passing over the lower

inverted trough in these situations. Nevertheless, in cases where the upper ridge is sufficiently far offshore to allow a northerly upper jet over the coastal zone, embedded shortwaves can lead to cyclogenesis there.

Diabatic generation of lower-tropospheric potential vorticity (PV) is related to the projection of the heating gradient onto the absolute vorticity vector. Thus, the vorticity-rich environment of the inverted coastal trough is favorable for lower-tropospheric PV generation in the presence of latent heating, owing to the increased magnitude of the absolute vorticity vector there (Raymond, 1992).

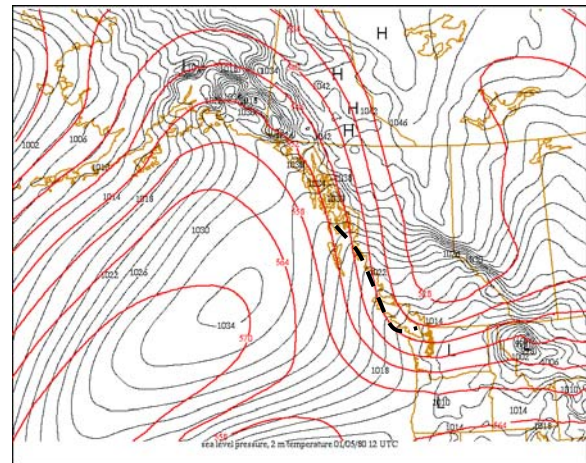


Figure 1. Analyzed 500-mb height (red, interval 6 dam) and sea level pressure (black, interval 2 hPa) valid 12 UTC 5 Jan 1980. Thick dashed line denotes inverted trough axis.

Here, we will utilize numerical model experiments to identify the relative importance of topography, diabatic processes, and upper-level dynamics during a representative coastal cyclone event that took place on 7–9 January 1980 is investigated in this study.

**2. DATA AND METHODS**

The North American Regional Reanalysis (NARR) dataset (Mesinger et al. 2006), featuring 32-km grid spacing, was used for analysis of this event. However the domain does

<sup>+</sup> Corresponding author address: Dr. Gary M. Lackmann, North Carolina State University, Dept. of Marine, Earth and Atmospheric Sciences, Raleigh, NC 27695. E-mail: gary@ncsu.edu

not extend far enough to the west to use for model initial and lateral boundary conditions for the 1980 event. Thus, NCAR/NCEP global reanalysis data, featuring 2.5° grid spacing, were used for model boundary conditions.

The Weather Research and Forecasting (WRF) model, version 2.1.2, was used for a control simulation and experiments in which terrain and the coastline were removed (the entire domain was set to water points). An additional experiment omitted latent heating.

### 3. CASE OVERVIEW

An arctic air mass moved southward from western Canada during the period from 5 to 7 Jan (Fig. 1), and cold air became established over western Washington State and interior sections of British Columbia by 00 UTC 7 Jan (not shown). Between 00 and 12 UTC 7 Jan, a cyclone formed to the west of southeast Alaska and coastal British Columbia (Fig. 2). Aloft, a shortwave trough was located far to the northwest of the surface cyclone at this time (Fig. 2). The cyclone was located beneath the left exit region of a jet streak at this time, evident at the 300-hPa level (Fig. 3).

The cyclone moved slowly southeastward after 12 UTC 7 Jan, and was located northwest of the Washington coast by 06 UTC 8 Jan (Fig. 4). A large upper trough is evident to the north of the surface cyclone at this time, with the surface low located in a favorable downstream position.

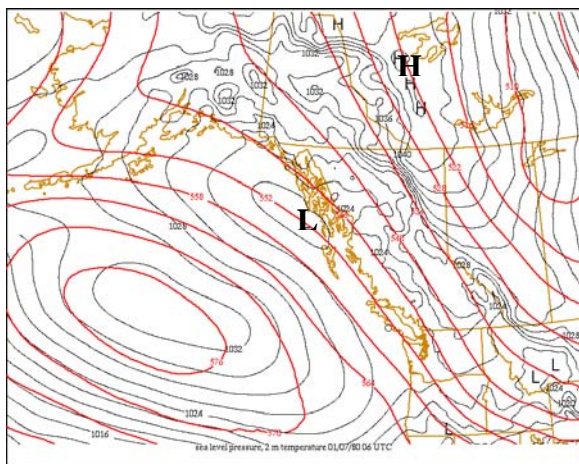


Figure 2. As in Fig. 1 except valid 06 UTC 7 Jan. “L” denotes location of the incipient coastal cyclone.

Steady snow began falling in western Washington during the afternoon of 7 Jan, and continued until early on 10 Jan (not shown). At Seattle-Tacoma Airport (SEA), 22 cm (8.5”) of snow was recorded during the event. By 11 Jan, a warmer marine airflow became established over the Pacific Northwest, ending the wintry weather event for interior sections of Washington and Oregon (not shown).

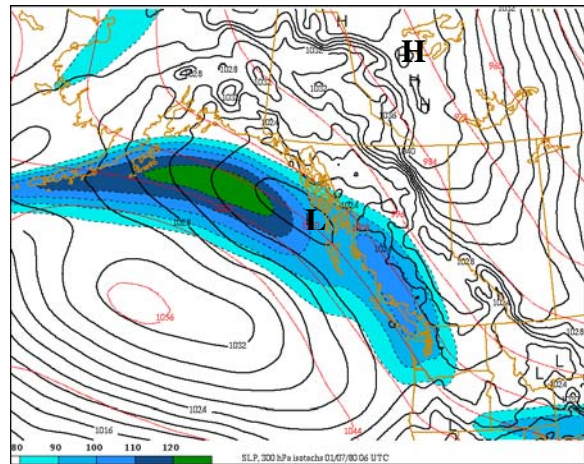


Figure 3. As in Fig. 2 except 300-hPa isotachs (kts, shaded) and heights (red solid contours, interval 12 dam) and sea level pressure (black contours, interval 2 hPa).

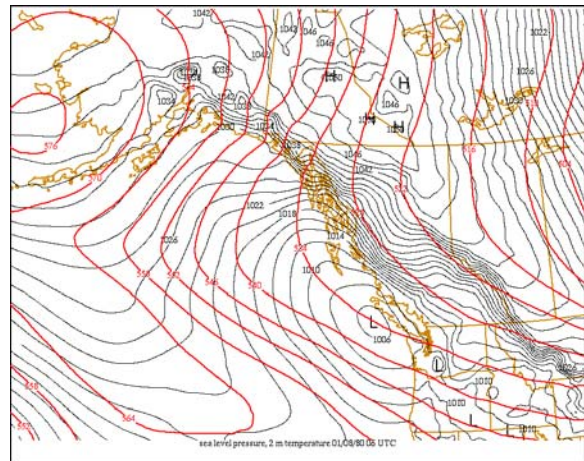


Figure 4. As in Fig. 1 except valid 06 UTC 8 Jan.

### 4. MODEL EXPERIMENTS

#### 4.1 Control

This event was simulated using the WRF model, initialized at 00 UTC 7 Jan and run for 60 hours (through 12 UTC 9 Jan). A grid spacing of 25 km was deemed sufficient to capture the main topographic features. Physics options included

the Lin microphysics scheme, the YSU boundary layer scheme, and Kain-Fritsch cumulus parameterization.

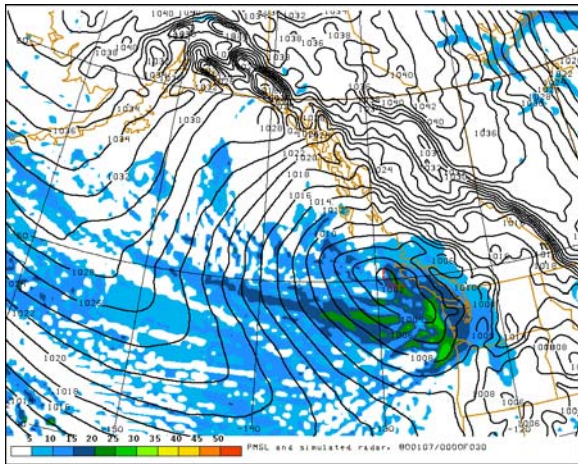


Figure 5. WRF model simulated radar (shaded) and sea level pressure (contour interval 2 hPa) for hour 30 of the control simulation valid 06 UTC 8 Jan.

The control simulation, despite the coarse ( $2.5^\circ$ ) initial conditions, was able to capture the cyclogenesis event in terms of both timing and location. Figure 5 shows the sea level pressure and model-simulated radar valid 06 UTC 8 Jan, and depicts a cyclone with a central pressure of  $\sim 1002$  hPa to the west of Vancouver Island. A reflectivity maximum extends westward from the low center, and precipitation associated with a warm front extends southeastward from the cyclone center. The model radar indicates precipitation spreading into western Washington state, closely matching surface observations from that time (Fig. 5).

The mobile upper trough moving southward across the Gulf of Alaska was characterized by a region of lower dynamic tropopause (defined as the 1.5 PVU surface) (Fig. 6). The leading edge of lowered tropopause over the Gulf of Alaska is aligned with the aforementioned precipitation feature (Fig. 5) as well as a lower-tropospheric PV maximum (Fig. 7). The lower tropospheric PV structure in the Gulf of Alaska was characterized by two east-west oriented PV maxima that likely were likely associated with diabatic processes, and PV streamers oriented perpendicular to the mountainous terrain of the Alaska coastline (Fig. 8). These PV streamers are likely frictionally produced.

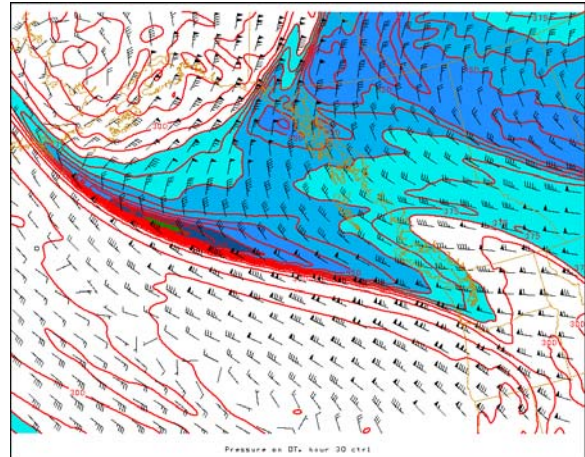


Figure 6. Pressure (interval 25 hPa) and winds on the dynamic tropopause from 30-h WRF model control simulation, valid 06 UTC 8 Jan.

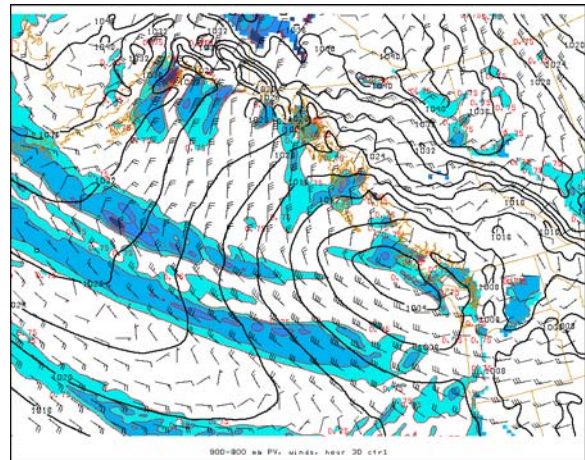


Figure 7. 800-900 hPa PV (PVU, shaded and contoured), 850-mb wind barbs, and sea level pressure (solid, interval 4 hPa) from 30-h WRF model control simulation valid 06 UTC 8 Jan.

#### 4.2 No terrain (NT) experiment

In an attempt to isolate the effects of terrain on this cyclone event, a simulation was run in which terrain was removed, and all points were set to water. Hereafter, we will refer to this model run as the no-terrain (NT) simulation. Using a modified version of the WRF Standard Initialization (WRFSI) package, we reduced the height of the terrain to 0 m everywhere. Some expectations include: (i) a weaker inverted coastal trough, and (ii) elimination of topographic PV streamers; these factors would tend to favor a weaker cyclone in the NT simulation. However, the reduction of

ageostrophic along-barrier channeling in the NT run should reduce mass convergence into the low center, contributing to a stronger cyclone in the NT simulation. Finally, by making all the points water, we expect that widespread shallow cloud and precipitation will form over interior sections of Canada where cold air resides.

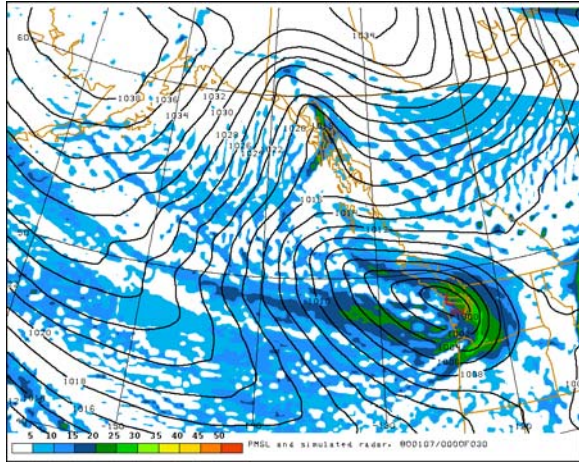


Figure 8. As in Fig. 5, except for NT model run.

Future experiments will include runs initialized prior to 00 UTC 7 Jan, because by then influence of terrain in setting up the coastal trough and baroclinic zone was already established.

Comparison of Figs. 5 and 8 demonstrates that the cyclone in the NT run is slightly ( $\sim 2$  hPa) stronger than in the control run at 06 UTC 8 Jan, and is located significantly farther east than that in the control run. This trend continues at 12 and 18 UTC 8 Jan, with the NT cyclone moving rapidly eastward across Washington state (not shown).

The lower-tropospheric PV structure differs between the runs as well, but primarily along the mountainous coastal regions, where no smaller-scale PV streamers are found in the NT simulation. An inverted trough is seen over southeastern Alaska, but this feature is evidently related to upper-level dynamics. As expected, the dynamic tropopause features are very similar between the NT and control runs (not shown).

#### 4.3 No latent heating experiment

An additional experiment that was identical to the control run, except for omission of latent

heat release (dubbed the NOLH run) was conducted with the purpose of determining the “dry dynamical” contribution to the cyclone event. Given the upper-level jet streak and trough in this case, we hypothesize that cyclogenesis will still take place in this run, but without diabatic processes, we anticipate a weaker system. However, owing to the fact that the diabatically produced lower-tropospheric PV anomalies with this system were not overly strong, the reduction in intensity may be modest. We further hypothesize that the PV streamers seen in the control run will again be present, if these features are indeed frictionally produced.

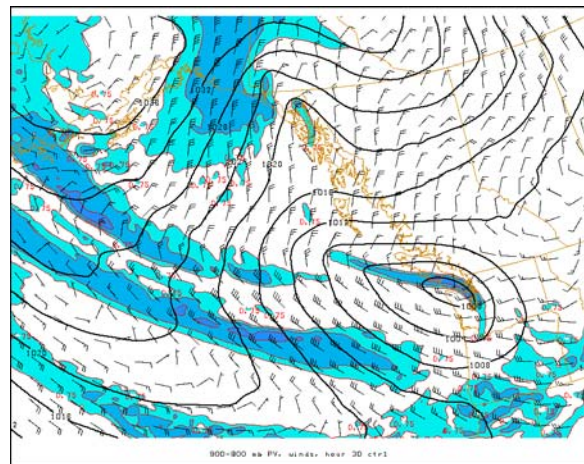


Figure 9. As in Fig. 7, except for NT model run.

Figure 10 presents the lower-tropospheric PV and sea-level pressure fields valid 06 UTC 8 Jan. The topographic PV banners are again apparent, and the cyclone is weaker. There are no pronounced lower PV maxima co-located with the cyclone center, however the east-west oriented PV feature seen over the Gulf of Alaska in the control and NT runs is again present, but rather than two strips, there is one. This suggests that this feature was either produced by latent heating prior to the start of the model run, or that it has an origin related to dry processes, for instance the downward extrusion of stratospheric air. Inspection of the lower PV field early in the run suggests that this feature forms due to deformation of a pre-existing PV maximum.

At 06 UTC 8 Jan, the central pressure of the NOLH cyclone is approximately 4 hPa higher

than that in the control run, and 8 hPa higher than in the NT simulation.

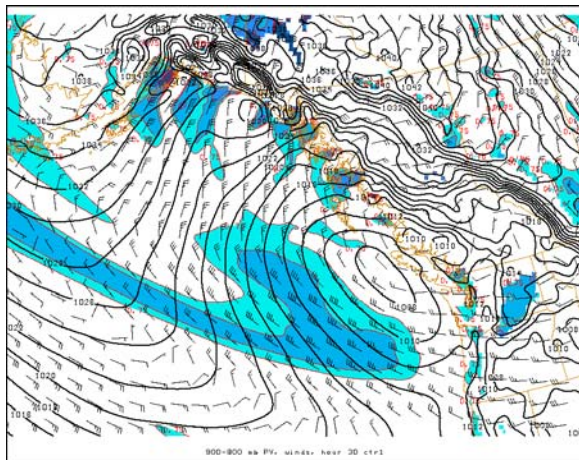


Figure 10. As in Fig. 7, except for NOLH model run, and contour interval 2 hPa.

## 5. CONCLUSIONS

A complex interaction of processes occurs during coastal cyclogenesis events that take place within an inverted, baroclinic trough that occasionally sets up along the west coast of North America during arctic air outbreaks. The goal of this research was to isolate the role of terrain and coastal processes relative to contributions from upper-tropospheric dynamics and diabatic processes for these events.

The control run was able to produce an accurate depiction of the cyclogenesis event, which took place initially in the left exit of an upper-level jet streak. Later, a mobile upper trough approached the surface cyclone from the north and the cyclone continued to deepen; the control simulation also accurately represented this process.

An experimental simulation in which terrain and the coastline were removed (NT) produced a system that was slightly stronger and located similarly through 7 Jan, but which moved eastward much faster than that in the control run on 8 Jan. The lower-tropospheric PV structure in the NT run was similar to that in the control except for the absence of PV streamers downwind of the terrain over the coastal areas of the Gulf of Alaska. This supports the hypothesis that these features are akin to the frictionally

generated PV banners discussed by Aebischer and Schär (1998) and others. If the model run had been initialized earlier, the differences between the control and NT simulations would likely have been greater, as the coastal baroclinic zone was already well-established by 00 UTC 7 Jan, when these runs were initialized.

A simulation in which latent heat was withheld produced the weakest cyclone of any of the 3 runs presented here, although the occurrence of cyclogenesis even in this run suggests that the upper-level dynamics were the dominant contributor to this event.

To summarize, the dynamics of this West Coast cyclone event are largely determined by an upper-air disturbance overtaking a pre-existing baroclinic zone and frontal trough. Non-negligible contributions from diabatic processes were found.

## 6. ACKNOWLEDGEMENTS

Support for this research was provided by North Carolina State University. The NARR data were obtained from the NCDC NOMADS server, and the WRF model was obtained from NCAR, which is sponsored by the NSF. Rob Fovell of UCLA is thanked for helpful program modifications that made it easier to remove terrain in the NT simulation.

## 7. REFERENCES

- Aebischer, U. and C. Schär, 1998: Low-level potential vorticity and cyclogenesis to the lee of the Alps. *J. Atmos. Sci.*, **55**, 186–207.
- Bailey, C. M., G. Hartfield, G. M. Lackmann, K. Keeter, and S. Sharp, 2003: An objective climatology, classification scheme, and assessment of sensible weather impacts for Appalachian cold-air damming. *Wea. Forecasting*, **18**, 641–661.
- Ferber, G. K., C. F. Mass, G. M. Lackmann, and M. W. Patnoe, 1993: Snowstorms over the Puget Sound Lowlands. *Wea. Forecasting*, **8**, 481–504.
- Lackmann, G. M., and J. Overland, 1989: Atmospheric structure and momentum balance during a gap-wind event in Shelikof Strait, Alaska. *Mon. Wea. Rev.*, **117**, 1817–1833.
- Mesinger, F. and co-authors, 2006: North American Regional Reanalysis. *Bull. Amer. Meteor. Soc.* **87**, 343–360.